Supplementary material

Cryogenic thermoelectric enhancements in $SbCl_3$-doped porous $Bi_{0.85}Sb_{0.15}$ alloys

Jian Wang,[a] Feng Luo,[a] Can Zhu,[a] Jiafu Wang,[a,b] Xiong He,[c] Yan Zhang,[d,e] Hongxia Liu,[d,e,*] Zhigang Sun[a,d,e,*]

[a] *State Key Laboratory of Advanced Technology for Materials Synthesis and Processing, Wuhan University of Technology, Wuhan 430070, China.*

[b] *School of Science, Wuhan University of Technology, Wuhan 430070, China.*

[c] *Hubei Engineering Research Center of Weak Magnetic-field Detection, College of Science, China Three Gorges University, Yichang 443002, China.*

[d] *School of Materials Science and Engineering, Taiyuan University of Science and Technology, Taiyuan 030024, China.*

[e] *Laboratory of Magnetic and Electric Functional Materials and the Applications, The Key Laboratory of Shanxi Province, Taiyuan 030024, China.*

* Corresponding author

Email: sun_zg@whut.edu.cn (Prof. Zhigang Sun) and hongxliu@126.com (Dr. Hongxia Liu)

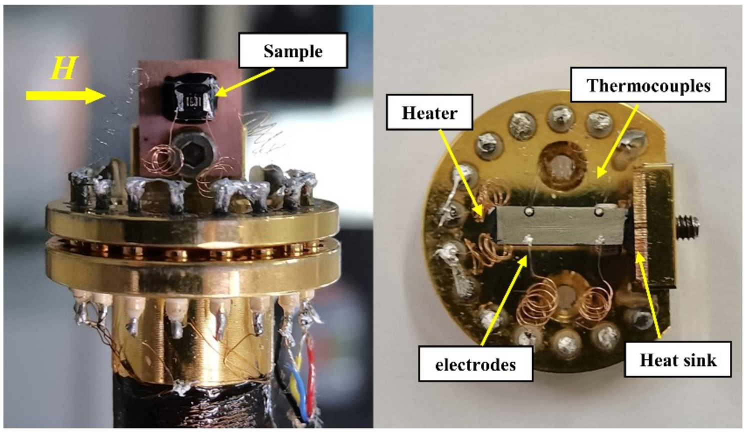

Fig.S1 Typical image of the sample mounting for TE parameters measurements.

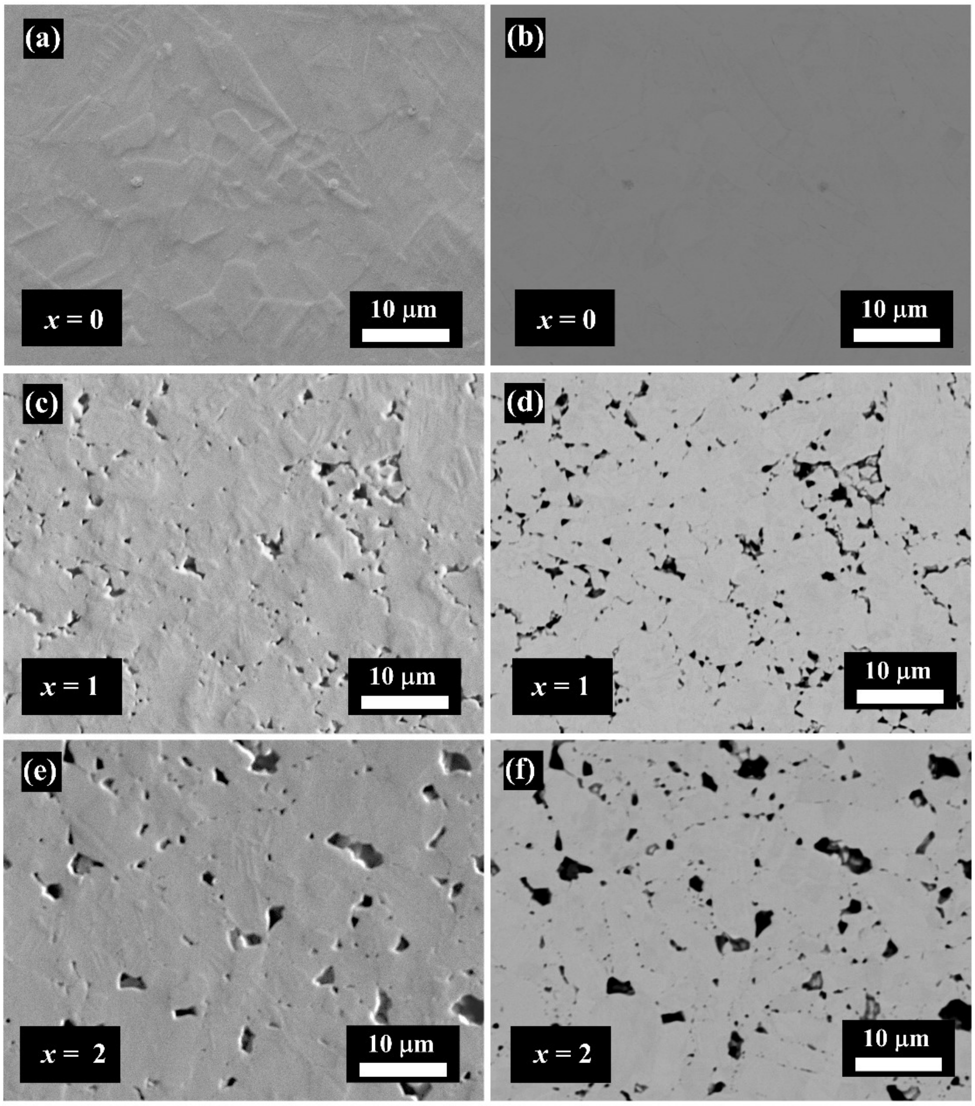

Fig. S2 (a, c, e) FESEM images and (b, d, f) corresponding BSE images of polished surface of the x = 0.5, 1, 2 sample, respectively.

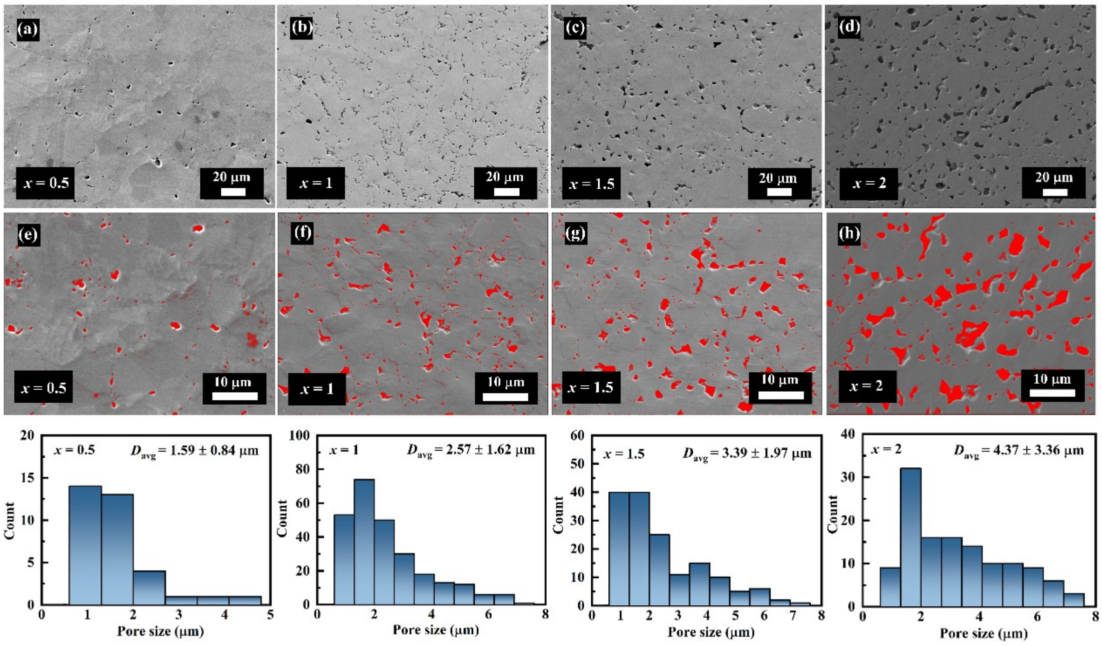

Fig. S3 (a-d) FESEM images of polished surface of the x = 0.5, 1, 1.5, 2 sample, respectively. (e-h) The built-in Pore size of the x = 0.5, 1, 1.5, 2 sample, respectively (The pores are filled with the red color to guide the eye).

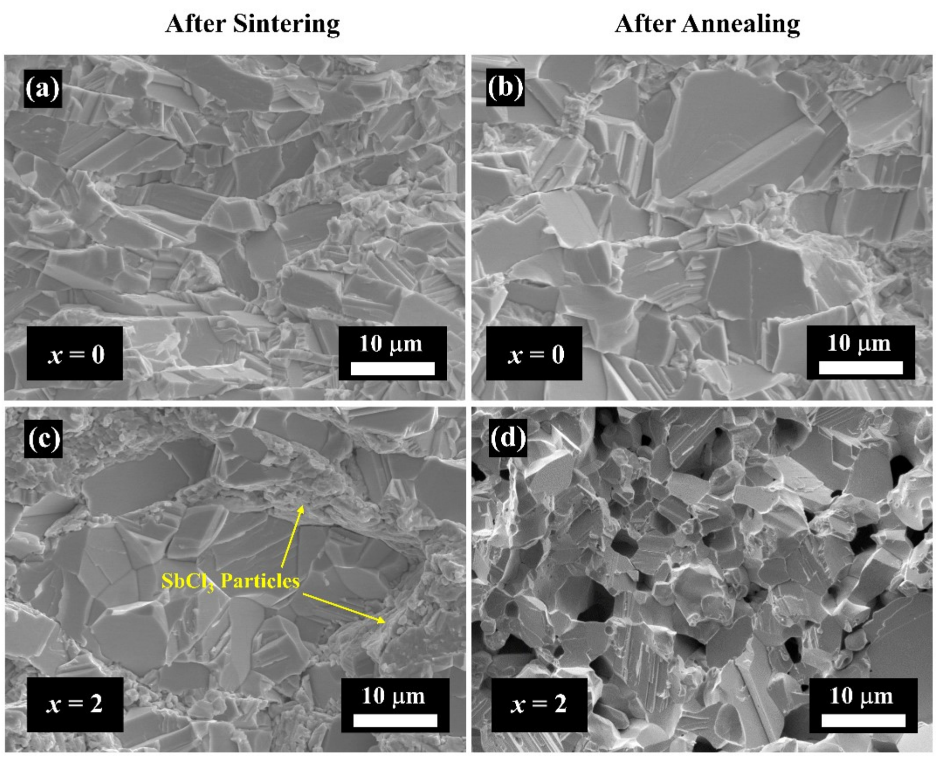

Fig. S4 FESEM images of fractured surface of (a, c) the sintered x = 0, 2 samples and (b, d) the annealed x = 0, 2 samples, respectively.

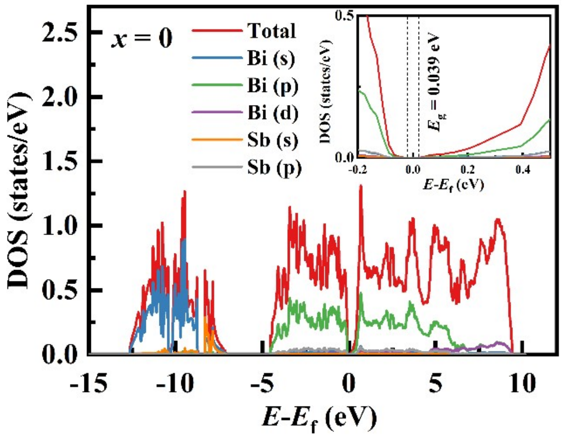

Fig. S5 The calculated projected electronic DOS of x = 0 sample.

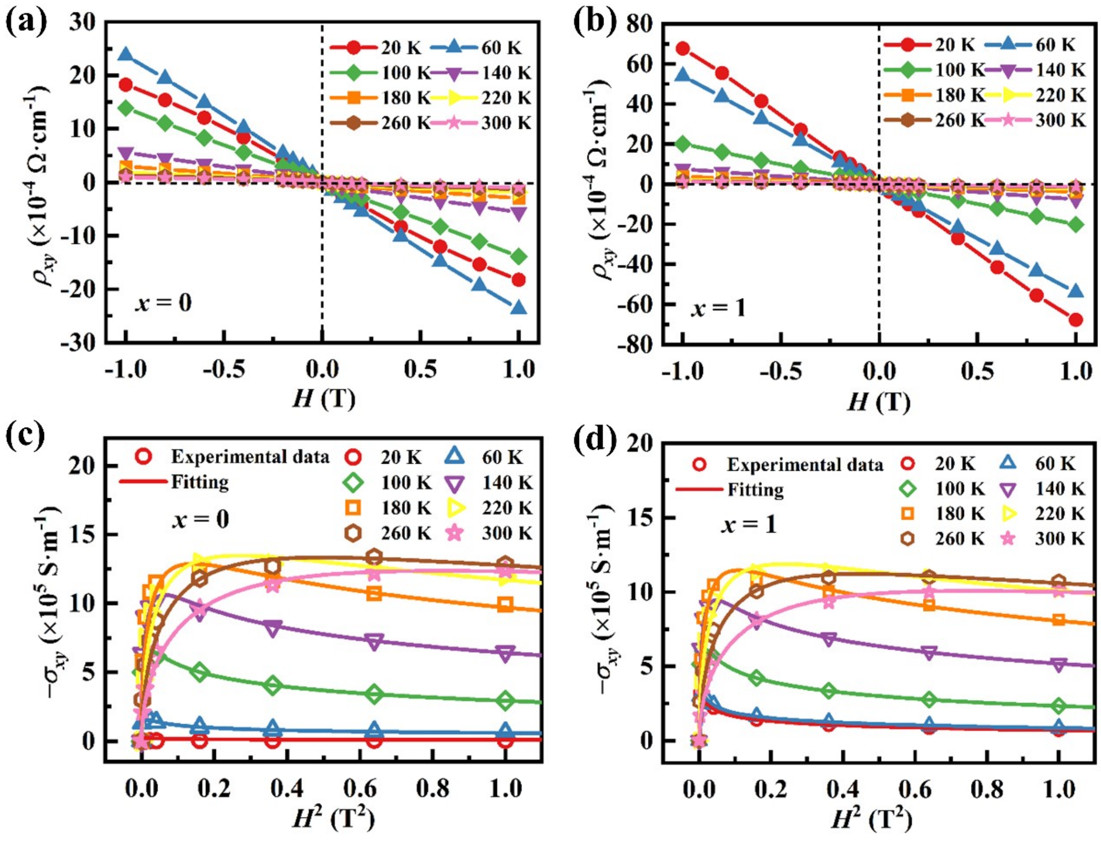

Fig.S6 Magnetic field dependence of (a,b) Hall resistivity and (c,d) magneto-conductivity at various temperature for x = 0 and x = 1 sample, respectively.

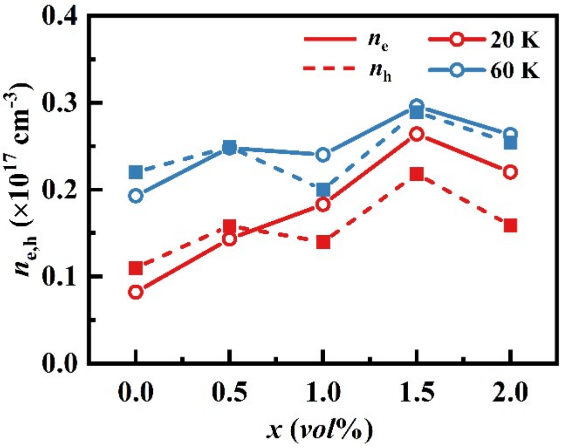

Fig.S7 Electron and hole concentration as a function of x at 20 and 60 K for $Bi_{0.85}Sb_{0.15}/x$ vol%$SbCl_3$ porous samples, respectively.

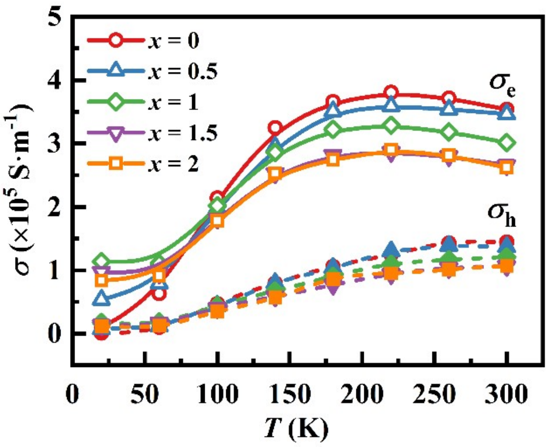

Fig.S8 Temperature dependence of partial electron (hole) conductivity of $Bi_{0.85}Sb_{0.15}/x$ vol%$SbCl_3$ porous samples.

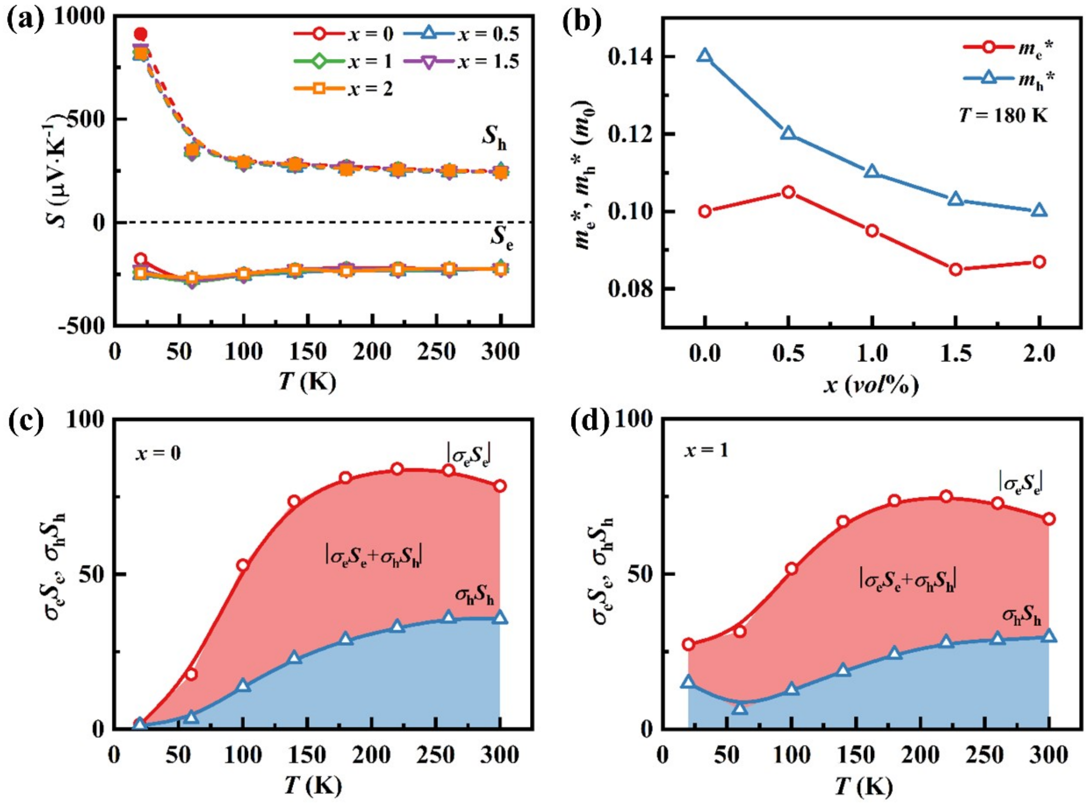

Fig.S9 (a) Temperature dependence of partial electron (hole) Seebeck coefficient of $Bi_{0.85}Sb_{0.15}$/*x vol*%$SbCl_3$ porous samples. (b) The estimated effective mass of electron and hole at 180 K. (c,d) Temperature dependence of ($\sigma_e S_e$, $\sigma_h S_h$) term for the $x = 0$ and $x = 1$ samples, respectively.

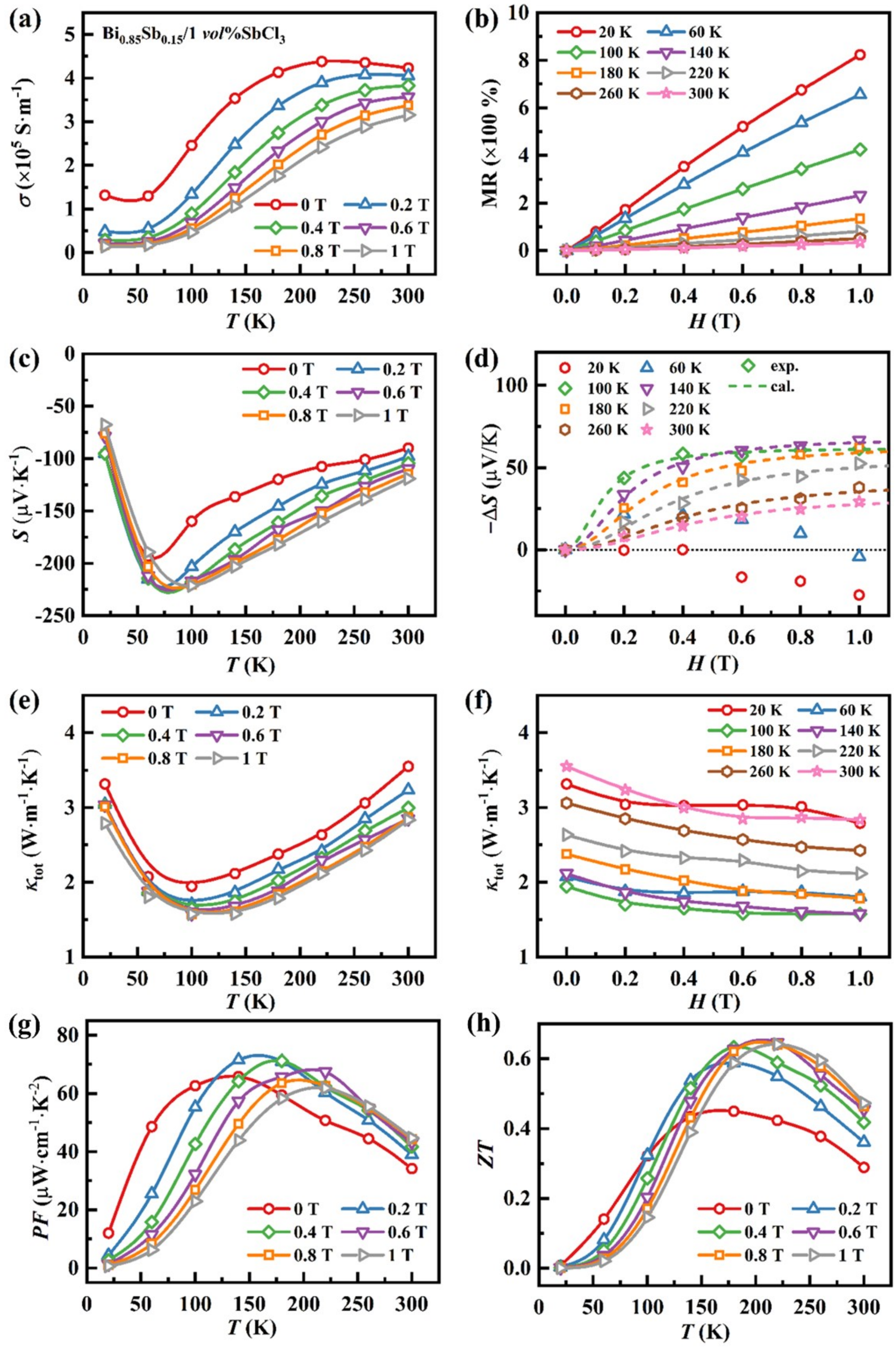

Fig.S10 Thermoelectric properties of $Bi_{0.85}Sb_{0.15}$/1 *vol*%$SbCl_3$ sample in the magnetic field of 0-1 T. Temperature dependence of (a) conductivity, (c) Seebeck coefficient, (e) thermal conductivity, (g) power factor, and (h) *ZT* values, respectively. Magnetic field dependence of (b) conductivity, (d) Seebeck coefficient, (f) thermal conductivity, respectively.

Transport properties analysis method

1. Details for the two band model

According to the semi-classical two-band model, the magneto-conductivity (σ_{xx}) in the systems with two kind carriers can be described by:[1,2]

$$\sigma_{xy}(H) = \frac{\rho_{xy}}{{\rho_{xx}}^2 + {\rho_{xy}}^2} \qquad \text{S1}$$

$$\sigma_{xy}(H) = \left[\frac{en_h{\mu_h}^2}{1 + {\mu_h}^2H^2} - \frac{en_e{\mu_e}^2}{1 + {\mu_e}^2H^2}\right]eB \qquad \text{S2}$$

$$\sigma(H = 0) = \sigma_e + \sigma_h \qquad \sigma_e = en_e\mu_e \qquad \sigma_h = en_h\mu_h \qquad \text{S3}$$

where n_e (or n_h) and μ_e (or μ_h) are the Hall carrier concentration and Hall mobility of electrons (or holes), respectively. σ_e and σ_h are the partial conductivity of electrons and holes, respectively. The n_e, n_h, μ_e, and μ_h at certain temperature can be deduced by fitting $\sigma \sim H$ curve with equation S1 and S2. For instance, Fig.S3c-d shows the magnetic field dependence of magneto-conductivity at various temperature and the curve fitting results for the $x = 0$ and $x = 1$ sample, respectively. It is observed that the $\sigma \sim H$ curves are well fitted by the two band model equations.

On basis of effective mass model, the transport coefficients can be determined by solving the Boltzmann Transport Equations with the relaxation assumption.[3,4] In two carrier system, the Seebeck coefficient can be expressed as:

$$S = \frac{\sigma_eS_e + \sigma_hS_h}{\sigma_e + \sigma_h} \qquad \text{S4}$$

where S_e is the partial Seebeck coefficient of electrons and S_h is the partial Seebeck coefficient of holes. The partial electron conductivity (σ_e) and partial hole conductivity (σ_h) can be obtained by equation S2.

The partial Seebeck coefficient of electrons and holes can respectively be expressed as:

$$S_e = -\left(\frac{k_B}{e}\right)\left(\frac{r + 5/2F_{r+3/2}(\eta_e)}{r + 3/2F_{r+1/2}(\eta_e)} - \eta_e\right)$$

$$S_h = (\frac{k_B}{e})(\frac{r + 5/2F_{r + 3/2}(\eta_e)}{r + 3/2F_{r + 1/2}(\eta_e)} - \eta_h) \quad \text{S5}$$

where k_B is the Boltzmann's constant, *e* is the electron charge, *r* is the scattering parameter of carriers (for the acoustic scattering mechanism, *r* equals to -1/2, while for the ionized impurity scattering mechanism, *r* equals to 3/2),[5] η_e is the reduced Fermi energy of the conduction band, and η_h is the reduced Fermi energy of the valence band, and *F* is the Fermi-Dirac integral.

The Fermi-Dirac integral can be expressed as:

$$F_i(\eta) = \int_0^\infty \frac{x^i dx}{1 + exp(x - \eta)} \quad \text{S6}$$

The relationship between the reduced Fermi energies of the conduction and valence bands is: $\eta_e + \eta_h = \eta_g$, where η_g is the reduced bandgap energy ($\eta_g = E_g/k_BT$). Since variation in E_g have effects on thermoelectric transport properties, a temperature dependent E_g is required for fully simulation of transport parameters. In our simulation, the E_g value of 14 meV at $T = 0$ K is used based on the result from $Bi_{0.85}Sb_{0.15}$ single crystal.[5] The temperature dependence of E_g can be obtained by the following equation:[6]

$$E_g(T) = E_g(0) + 2.25/(\exp(60/T) - 1) \quad \text{S7}$$

The carrier concentration of electrons (n_e) and holes (n_h) can be expressed as:

$$n_e = 4\pi\left(\frac{2m_e^* k_BT}{h^2}\right)^{3/2}F_{1/2}(\eta_e) \qquad n_h = 4\pi\left(\frac{2m_h^* k_BT}{h^2}\right)^{3/2}F_{1/2}(\eta_h) \quad \text{S8}$$

where m_e^* and m_h^* are the density of states effective mass of electrons and holes, respectively, and *h* is the Planck's constant.

The weighted mobility can be expressed as:[7]

$$\mu_w = \frac{3h^3\sigma}{8\pi e(2m_e^* k_BT)^{3/2}}\left[\frac{\exp\left[\frac{|S|}{k_B/e} - 2\right]}{1 + \exp\left[-5\left(\frac{|S|}{k_B/e} - 1\right)\right]} + \frac{\frac{3}{\pi^2}\frac{|S|}{k_B/e}}{1 + \exp\left[5\left(\frac{|S|}{k_B/e} - 1\right)\right]}\right] \quad \text{S9}$$

For the thermal conductivity, the electronic thermal conductivity (κ_{ele}), lattice thermal conductivity (κ_L), and bipolar thermal conductivity (κ_{bip}) are considered in the two band model.[8] According to the Wiedemann-Franz relation, κ_{ele} is defined as $\kappa_{ele} = L\sigma T$, where Lorenz number L for the electrons (L_e) and holes (L_h) can be respectively expressed as:

$$L_e = (\frac{k_B}{e})^2[\frac{r + 7/2F_{r+5/2}(\eta_e)}{r + 3/2F_{r+1/2}(\eta_e)} - (\frac{r + 5/2F_{r+3/2}(\eta_e)}{r + 3/2F_{r+1/2}(\eta_e)})^2]$$

$$L_h = (\frac{k_B}{e})^2[\frac{r + 7/2F_{r+5/2}(\eta_h)}{r + 3/2F_{r+1/2}(\eta_h)} - (\frac{r + 5/2F_{r+3/2}(\eta_h)}{r + 3/2F_{r+1/2}(\eta_h)})^2]$$

S10

Thus, the κ_e, κ_{bip} and the total thermal conductivity can be expressed as:

$$\kappa_{ele} = L_e\sigma_e T + L_h\sigma_h T \tag{S11}$$

$$\kappa_{bip} = (\frac{\sigma_e\sigma_h}{\sigma_e + \sigma_h})(S_e - S_h)^2 T \tag{S12}$$

$$\kappa_{tot} = \kappa_{ele} + \kappa_L + \kappa_{bip} \tag{S13}$$

2. Debye-Callaway model for calculating the lattice thermal conductivity

According to the Debye-Callaway model,[9-11] κ_L can be expressed as a sum of the spectral lattice thermal conductivity $\kappa_S(f)$ from different frequencies (f):

$$\kappa_L = \int \kappa_S(f)df = \frac{1}{3}\int_0^{f_D} C_S(f)v_g(f)^2\tau_{tot}(f)df \tag{S14}$$

The κ_S (f) is determined by the spectral heat capacity $C_S(f)$, the phonon group velocity $v_g(f)$, and the total relaxation time $\tau_{tot}(f)$. For simple approximation, $v_g(f)$ is assumed as a constant value v_s (sound velocity). The Debye frequency f_D can be expressed as:

$$f_D = \frac{k_B\theta_D}{\hbar} = (\frac{6\pi^2 N}{V})^{1/3}v_S \tag{S15}$$

where θ_D is Debye temperature, N is the number of atoms in a unit cell volume, V is the unit-cell volume, k_B is the Boltzmann constant and $\hbar$ is the reduced Plank constant. The $C_S(f)$ can be expressed as:

$$C_S(f) = \frac{3k_B f^2}{2\pi^2 {v_S}^2} \tag{S16}$$

Thus, κ_L and κ_S are expressed as:

$$\kappa_L = \frac{3k_B f^2}{2\pi^2 v_S}(\frac{k_B T}{\hbar})^3 \int_0^{\theta_D/T} \tau_{tot}(x) \frac{x^2 exp(x)}{[\exp(x) - 1]^2} df \tag{S17}$$

$$\kappa_S = \frac{k_B}{2\pi^2 v_S}(\frac{k_B T}{\hbar})^3 \tau_{tot}(x) \frac{x^2 exp(x)}{[\exp(x) - 1]^2} \tag{S18}$$

where $x = \hbar f / k_B T$ is the reduced phonon frequency. According to Matthiessen's rule, $\tau_{tot}(x)$ is the reciprocal sum of the relaxation times from different phonon scattering mechanisms including the Umklapp phonon-phonon scatterings (U), normal phonon-phonon scatterings (N), grain boundaries scatterings (B), point defects scatterings (PD), and nano-precipitates phonon scatterings (NP). For our porous sample, the pores are regarded as the precipitates, and the predominant phonon scattering mechanisms including U, N, B and NP are considered. So, τ_{tot} is calculated by

$$ {\tau_{tot}}^{-1} = {\tau_U}^{-1} + {\tau_N}^{-1} + {\tau_B}^{-1} + {\tau_{NP}}^{-1} + \ldots \tag{S19}$$

The τ_U^{-1} is calculated by

$$ {\tau_U}^{-1} = \frac{\hbar \gamma^2 f^2 T}{M_{av} {v_S}^2 \theta_D} \exp(-\frac{\theta_D}{3T})$$

where M_{av} and γ are the average atomic mass and Grüneisen parameter respectively. The τ_N^{-1} can be simply expressed as τ_U^{-1} with an additional factor β, as

$$ {\tau_N}^{-1} = \beta {\tau_U}^{-1} \tag{S20}$$

The τ_B^{-1} is calculated by

$$ {\tau_B}^{-1} = \frac{v_S}{D} \tag{S21}$$

where D is the average grain size of polycrystalline materials.

The τ_{NP}^{-1} is calculated by

$$\tau_{NP}^{-1} = [(2\pi R_{NP}^{2})^{-1} + (\pi R_{NP}^{2}\frac{4}{9}(\frac{\Delta\rho}{\rho})^{2}(\frac{fR_{NP}}{v_S})^{4})^{-1}]^{-1}N_{NP} \quad \text{S22}$$

where R_{NP} and N_{NP} are the radius and number density for the pores, ρ and $\Delta\rho$ are the matrix density and density difference between the pore and matrix. The parameters for modeling κ_L in this work are shown in Table S1.

Table.S1 Parameters for modeling the lattice thermal conductivity of $Bi_{0.85}Sb_{0.15}/x$ *vol*%$SbCl_3$ porous materials. The lattice parameter used for the calculation is the lattice constant of rhombohedral unit cell transformed by hexagonal unit cell.

Parameters	Values
Grüneisen parameter γ	1.2[12]
Sound velocity vs ($m \cdot s^{-1}$)	1179[13]
Transverse sound velocity vt ($m \cdot s^{-1}$)	1050[13]
Longitudinal sound velocity vl ($m \cdot s^{-1}$)	2123[13]
Debye temperature θ_D (K)	120[13]
Lattice parameter a (Å)	4.7205 (this work)
Average atomic mass Mav (kg)	3.28×10^{-25}
Grain size D (μm)	25 (this work)

Matrix density ρ ($g \cdot cm^{-3}$)	9.25 (this work)
Density difference between matrix and pores $\Delta\rho$ (g·cm–3)	7.96
Mean radius for the micropores (μm)	1(fitted)
Number density of micropores (m^{-3})	7.98×10^{-18} (fitted)

References:

1. W. Liu, Z. Wang, J. Wang, H. Bai, Z. Li, J. Sun, X. Zhou, J. Luo, W. Wang, C. Zhang, J. Wu, Y. Sun, Z. Zhu, Q. Zhang, X. Tang, Adv. Funct. Mater, 2022, 32, 2202143.
2. Z. Chen, X. Zhang, J. Ren, Z. Zeng, Y. Chen, J. He, L. Chen, Y. Pei, Nat. Commun, 2021, 12, 3837.
3. V. Jovovic, J. P. Heremans, Phys. Rev. B, 2008, 77, 245204.
4. Y. Hasegawa, Y. Ishikawa, T. Saso, H. Shirai, H. Morita, T. Komine, H. Nakamura, Physica B, 2006, 382, 140-146.
5. S. Gao, J. Gaskins, X. Hu, K. Tomko, P. Hopkins, S. J. Poon, Sci Rep, 2019, 9, 14892.
6. N. M. Ravindra, V. K. Srivastava, J. Phys. Chem. Solids, 1980, 41, 1289-1290.
7. G. J. Snyder, A. H. Snyder, M. Wood, R. Gurunathan, B. H. Snyder, C. Niu, Adv. Mater., 2020, 32, 2001537.
8. M. Otsuka, R. Homma, Y. Hasegawa, J. Electron. Mater., 2017, 46, 2752-2764.
9. J. Callaway, H. C. von Baeyer, Physical Review, 1960, 120, 1149.
10. C. Zhu, F. Luo, J. Wang, S. Zhang, J. Wang, H. Liu, Z. Sun, J. Mater. Chem. C, 2022, 10, 9052-9061.

11. T. K. Dey, K. D. Chaudhuri, Journal of Low Temperature Physics, 1976, 23, 419-426.
12. G. K. White, Journal of Physics C: Solid State Physics, 1972, 5, 2731.
13. S. Singh, I. Valencia-Jaime, O. Pavlic, A. H. Romero, Phys. Rev. B, 2018, 97, 11.